Long-Range Ferromagnetic Dipolar Ordering of High-Spin Molecular Clusters

A. Morello,[1] F. L. Mettes,[1] F. Luis,[2] J. F. Fernández,[2] J. Krzystek,[3] G. Aromí,[4] G. Christou,[5] and L. J. de Jongh[1,*]

[1]*Kamerlingh Onnes Laboratory, Leiden Institute of Physics, Leiden University, P.O. Box 9504, 2300 RA Leiden, The Netherlands*
[2]*Instituto de Ciencia de Materiales de Aragón, CSIC-Universidad de Zaragoza, 50009 Zaragoza, Spain*
[3]*National High Magnetic Field Laboratory, Tallahassee, Florida 32310*
[4]*Gorlaeus Laboratories, Leiden Institute of Chemistry, Leiden University, P.O. Box 9502, 2300 RA Leiden, The Netherlands*
[5]*Department of Chemistry, University of Florida, Gainesville, Florida 32611*

We report the first example of a transition to long-range magnetic order in a purely dipolarly interacting molecular magnet. For the magnetic cluster compound $Mn_6O_4Br_4(Et_2dbm)_6$, the anisotropy experienced by the total spin $S = 12$ of each cluster is so small that spin-lattice relaxation remains fast down to the lowest temperatures, thus enabling dipolar order to occur within experimental times at $T_c = 0.16$ K. In high magnetic fields, the relaxation rate becomes drastically reduced and the interplay between nuclear- and electron-spin lattice relaxation is revealed.

Few examples of long-range magnetic order induced by purely dipolar interactions are known as yet [1,2]. Therefore, the possibility to study such phase transitions and the associated long-time relaxation phenomena in detail in high-spin molecular cluster compounds, with varying crystalline packing symmetries and different types of anisotropy, presents an attractive subject [3]. However, for the most extensively studied molecular clusters so far, such as Mn_{12}, Fe_8, and Mn_4 [4–7], the uniaxial anisotropy experienced by the cluster spins is very strong. Consequently, the electronic spin-lattice relaxation time T_1^{el} becomes very long at low temperatures and the cluster spins become frozen at temperatures of the order of 1 K, i.e., much higher than the ordering temperatures $T_c \sim 0.1$ K expected on the basis of the intercluster dipolar couplings [3]. Although quantum tunneling of these cluster spins has been observed [4–7], and could in principle provide a relaxation path towards the magnetically ordered equilibrium state [3], the associated rates in zero field are extremely small (< 100 Hz). For these systems, tunneling becomes effective only when strong transverse fields B_t are applied to increase the tunneling rate. Although the tunability of this rate and thus of T_1^{el} by B_t could recently be demonstrated for Mn_{12}, Fe_8, and Mn_4 [7], no ordering has yet been observed.

The obvious way to obtain a dipolar molecular magnet is thus to look for a high-spin molecule having sufficiently weak magnetic anisotropy and negligible *intercluster* superexchange interactions. Here we report data for $Mn_6O_4Br_4(Et_2dbm)_6$, hereafter abbreviated as Mn_6 [8]. The molecular core of Mn_6 is a highly symmetric octahedron of Mn^{3+} ions (with spin $s = 2$) that are ferromagnetically coupled via strong *intracluster* superexchange interactions (Fig. 1). Accordingly, the ground state is a $S = 12$ multiplet and the energy of the nearest excited state is approximately 150 K higher [8]. The unit cell is monoclinic, with space group Pc, and contains four molecules [9] bound together only by van der Waals

forces. Intercluster superexchange is therefore negligible and only dipolar interactions couple the cluster spins. The net magnetocrystalline anisotropy of this cluster proves to be sufficiently small to enable measurements of its equilibrium magnetic susceptibility and specific heat down to our lowest temperatures (15 mK).

The main results of this paper follow. We have observed that the magnetic clusters do undergo a transition to a long-range ferromagnetically ordered state at $T_c = 0.161(2)$ K. This transition can be observed within experimental times (1–100 s) because the magnetic relaxation is not too slow at very low temperatures. We have obtained further information on the magnetic relaxation by applying a magnetic field. It turns out that the relaxation rate vanishes exponentially as the field increases. The interplay between nuclear- and electron-spin lattice relaxation is also revealed.

Polycrystalline samples of Mn_6 were prepared as in Ref. [9]. The specific heat of a few milligrams of sample, mixed with Apiezon grease, was measured at low-T in a homemade calorimeter [7] that makes use of the thermal
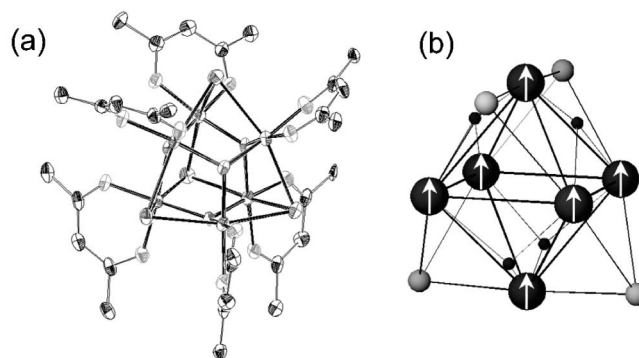

FIG. 1. (a) Crystal structure of $Mn_6O_4Br_4(Et_2dbm)_6$ [8]; (b) detail of the symmetric octahedral core, containing six ferromagnetically coupled Mn^{3+} ions, yielding a total spin $S = 12$ for this molecular superparamagnetic particle.

relaxation method. An important advantage of this method is that the characteristic time τ_e of the experiment (typically, $\tau_e \simeq 1$–100 seconds at low-T) can be varied by changing the dimensions (and therefore the thermal resistance) of the Au wire that acts as a thermal link between the calorimeter and the mixing chamber of the ^{3}He-^{4}He dilution refrigerator. The ac susceptibility data were taken between 0.015 and 4 K with a mutual inductance bridge. The frequency was varied from 230 to 7700 Hz. Magnetic data for $T > 1.8$ K were taken with a SQUID magnetometer.

We first discuss the magnitude of the anisotropy. The spin Hamiltonian for the molecule is

$$\mathcal{H} = -DS_z^2 - g\mu_B \vec{B} \cdot \vec{S}. \tag{1}$$

Previously published magnetic data for $T > 1.8$ K already indicated an upper limit of about 0.01 K for D/k_B [8]. In order to obtain an independent estimate of D, high-frequency ESR data were taken in the range 95–380 GHz. Owing to the combination of very small D and large S, as well as the presence of a signal at $g = 2.00$ arising from a minute amount of Mn^{2+} impurity (often seen in ESR of Mn^{3+} compounds), the interpretation of the spectra was not fully conclusive. Nevertheless, signals with a clearly visible structure on the low-field end of the spectra could be obtained. It could be identified as fine structure originating from zero-field splitting (ZFS), since it was independent of field and frequency. Simulations of the spectra performed using Eq. (1) agree well with the experiment taking $|D|/k_B \sim 0.03$ or ~ 0.05 K, depending on the sign of D (which could not be unequivocally determined). Although a smaller rhombic component could be present, the data do not justify a more elaborate fitting.

The isotropic character of the molecular spin might seem paradoxical at first, considering that the individual Mn^{3+} ions, being Jahn-Teller ions, experience strong anisotropy. However, the spin Hamiltonian for the cluster is determined by the vectorial addition of the local tensors of the individual atoms, which can give rise to a low net anisotropy for highly symmetric molecules such as Mn_6 (cf. Fig. 1), no matter how large the ZFS of the constituting atoms [10]. In fact, the possibility to tune the net anisotropy of the cluster spin is one of the attractive properties of molecular superparamagnets.

As first evidence for ordering of the magnetic moments we show zero-field ac susceptibility data in Fig. 2. The real part χ' shows a sharp maximum at $T_c = 0.161(2)$ K. We found that χ' at T_c is close to the estimated limit for a ferromagnetic powder sample, $1/(\rho N_s + \rho_{sam} N_c) \simeq 0.14 \pm 0.02$ emu/g, where $\rho = 1.45$ g/cm^3 and $\rho_{sam} \simeq 0.45$ g/cm^3 are, respectively, the densities of bulk Mn_6 and of the powder sample, $N_s = 4\pi/3$ is the demagnetizing factor of a crystallite, approximated by a sphere, and $N_c \simeq 2.51$ is the demagnetizing factor of the sample holder. This indicates that Mn_6 is ferromagnetically or-
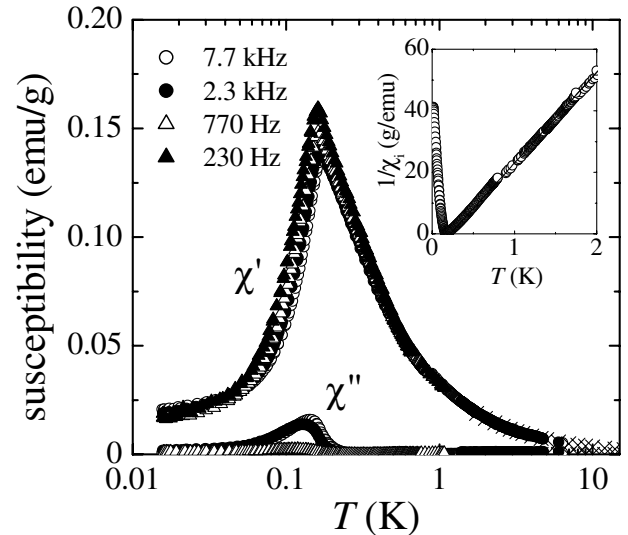

FIG. 2. The ac susceptibility of Mn_6 at zero field and four different frequencies. Data measured above 1.8 K in a commercial SQUID magnetometer are also shown ($\times$). Inset: χ' corrected for demagnetization effects. The full line shows the best fit of a Curie-Weiss law to the data for $T > 0.3$ K, yielding $\theta = 0.20(3)$ K.

dered below T_c. Susceptibility data χ_i corrected for the demagnetizing field $(\chi_i = \chi'/[1 - (\rho N_s + \rho_{sam} N_c)\chi'])$ follow the Curie-Weiss law $\chi = C/(T - \theta)$ down to approximately 0.3 K, with $C = 0.034(1)$ cm^3 K/g and $\theta = 0.20(3)$ K. The constant C equals, within the experimental errors, the theoretical value for randomly oriented crystals with Ising-like anisotropy $N_A g^2 \mu_B^2 S(S + 1)/3k_B P_m = 0.0332$ cm^3 K/g, where $S = 12$, $g = 2$, and the molecular weight $P_m = 2347.06$. The positive θ confirms the ferromagnetic nature of the ordered phase. From the mean-field equation $\theta = 2zJ_{eff}S(S + 1)/3k_B$, we estimate the effective intercluster magnetic interaction $J_{eff} \approx 1.6 \times 10^{-4}$ K, and the associated effective field $H_{eff} = 2zJ_{eff}S/g\mu_B = 3.5 \times 10^2$ Oe coming from the $z = 12$ nearest neighbors.

The maximum value of χ' is seen to vary only weakly with ω, which we attribute to the anisotropy. The total activation energy of Mn_6 amounts to $DS^2 \approx 1.5$ K; i.e., it is about 45 times smaller than for Mn_{12}. Accordingly, one expects the superparamagnetic blocking of the Mn_6 spins to occur when $T \simeq T_B(Mn_{12})/45$, that is, below $\simeq 0.12$ K. In other words, for $T \to T_c$, the approach to equilibrium begins to be hindered by the anisotropy of the individual molecular spins. We stress, however, that the frequency dependence of χ' observed here is very different from that of the well-known anisotropic superparamagnetic clusters or that of spin glasses. Below T_c, χ' decreases rapidly, as expected for an anisotropic ferromagnet in which the domain-wall motions become progressively pinned. The associated domain-wall losses should then lead to a frequency dependent maximum around T_c in the imaginary part, χ'', as seen experimentally. Indeed, although

the Mn_6 spins can be considered as nearly isotropic at high temperatures, the anisotropy energy ($\simeq 2DS$) is of the same order as the dipolar interaction energy $\mu^2/r^3 \simeq 0.1$ K between nearest neighbor molecules. Thus the ordering should be that of an Ising dipolar ferromagnet.

Additional evidence for the ferromagnetic transition at T_c is provided by the electronic specific heat c_e [11], shown in Fig. 3, which reveals a sharp peak at 0.15(2) K. Numerical integration of c_e/T between 0.08 and 4 K gives a total entropy change of about $3.4k_B$ per molecule, very close to the value for a fully split $S = 12$ spin multiplet (i.e., $k_B \ln(2S + 1) = 3.22k_B$). We thus may attribute the peak to the long-range order of the molecular spins. We note, however, that at T_c the entropy amounts to about $1k_B$ per spin, showing that only the lowest energy spin states take part in the magnetic ordering.

We have performed Monte Carlo (MC) simulations for an $S = 12$ Ising model of magnetic dipoles on an orthorhombic lattice with axes $a_x = 15.7$ Å, $a_y = 23.33$ Å, and $a_z = 16.7$ Å, which approximates the crystal structure of Mn_6. The model includes dipolar interactions as well as the anisotropy term $-DS_z^2$ given in Eq. (1). Neglecting interactions, the ZFS of the $S = 12$ multiplet produced by this crystal field term lead to a Schottky anomaly in c_e, as shown by the dotted curve in Fig. 3. The fit in the range above 0.5 K yields $D/k_B \simeq 0.013$ K, in good agreement with our previous estimates. The intermolecular dipolar interactions remove the remaining degeneracy of the $|\pm m\rangle$ spin doublets. The MC simulations show that the ground state is ferromagnetically ordered, as observed, and predict a shape for c_e that is in very good agreement with the experiment. In Fig. 3, we show c_e calculated assuming all molecular easy (z) axes to point along a_z,

i.e., one of the two nearly equivalent short axes of the actual lattice. Similar results were obtained for other orientations chosen for the anisotropy (z) axis. We note that the Ising simulations give $T_c = 0.22$ K, which is slightly higher than the experimental $T_c = 0.161(2)$ K. This difference may be related to the finite value of the anisotropy. Model calculations for this crystal structure, assuming classical anisotropic Heisenberg spins with varying anisotropy [12], show that different ferromagnetic ground states are possible, depending on the competition between local crystal field effects and long-range dipolar interactions. The variation of T_c with anisotropy, as well as the form of the calculated and observed specific heat anomaly, are specific for dipolar interactions, and differ widely from the analogs for the usual superexchange ferromagnets [13].

We next turn to the specific heat data obtained in varying magnetic field B, plotted in Fig. 4. Even for the lowest B value, the ordering anomaly is fully suppressed, as expected for a ferromagnet [13]. Accordingly, we may account for these data with the Hamiltonian (1) neglecting dipolar interactions. The Zeeman term splits the otherwise degenerate $|\pm m\rangle$ doublets, and already for $B \sim 0.5$ T the level splittings become predominantly determined by B, so that the anisotropy term can also be neglected. As seen in Fig. 4, the calculations performed with $D = 0$ reproduce the data quite satisfactorily at higher temperatures (dotted curves).

However, when the maxima of the Schottky anomalies are shifted to higher T by increasing B, an additional contribution at low T is revealed. It is most clearly visible
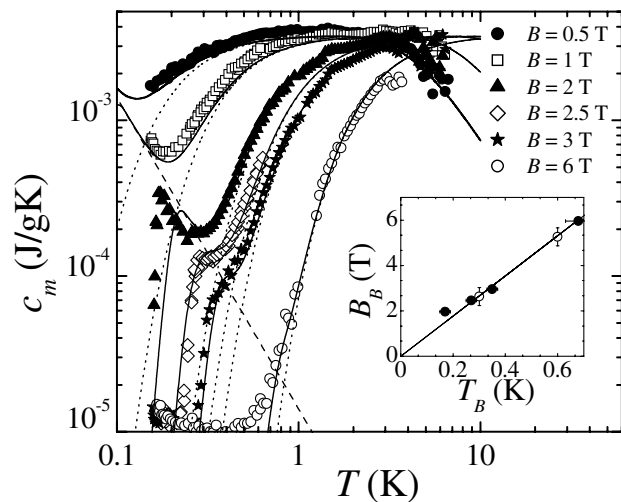
FIG. 4. Magnetic specific heat of Mn_6 for various applied fields. Dotted and dashed lines: calculated equilibrium specific heats of the electronic and the nuclear spins, respectively. Full lines: Time-dependent total specific heat calculated taking into account the nuclear spin-lattice relaxation. Inset: Magnetic field B_B needed to take the nuclear spins off-equilibrium. ○, obtained from c_{nucl} vs B isotherms; ●, from c_{nucl} vs T at constant field.
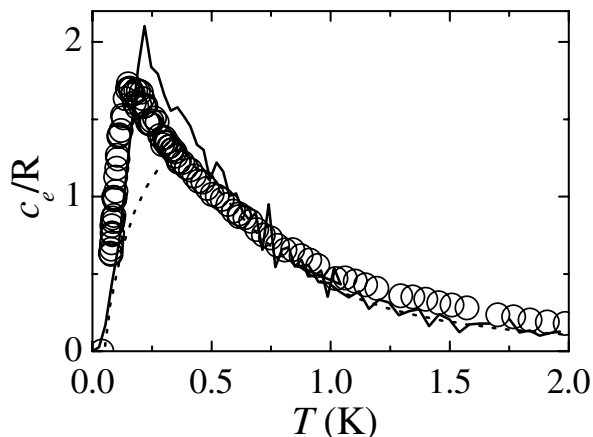
FIG. 3. Electronic specific heat data (○) of Mn_6 at zero field. The dotted line is the Schottky anomaly calculated with $D = 0.013$ K. The full line is the Monte Carlo (MC) calculation for an orthorhombic lattice of 1024 Ising spins with periodic boundary conditions. For each point, we performed 2×10^4 MC steps per spin.

in the curves for $1\,\mathrm{T} < B < 2.5\,\mathrm{T}$, and varies with temperature as $cT^2/R = 4 \times 10^{-3}$. We attribute this to the high-temperature tail of the specific heat contribution c_{nucl} arising from the Mn nuclear spins ($I = 5/2$), whose energy levels are split by the hyperfine interaction with the Mn^{3+} electronic spins s. This interaction can be approximated by $\mathcal{H}_{\mathrm{hf}} = sA_{\mathrm{hf}}m_I$, where A_{hf} is the hyperfine constant and m_I is the projection of the nuclear spin along the electronic spin. At high temperatures (i.e., when $A_{\mathrm{hf}}s \ll k_B T$) $c_{\mathrm{nucl}}/R \simeq \frac{1}{3}A_{\mathrm{hf}}^2 s^2 I(I+1)T^{-2}$ [14]. Taking $A_{\mathrm{hf}} = 7.6\,\mathrm{mK}$ as used previously to simulate ESR spectra measured on a Mn_4 cluster [15], we obtain the dashed line of Fig. 4. This contribution was subtracted from the zero-field data shown in Fig. 3.

A remarkable feature of the experimental data that is not reproduced by these calculations is that, at the lowest T, the nuclear specific heat drops abruptly to about $10^{-5}\,\mathrm{J/g\,K}$. The temperature T_B where the drop occurs depends on B but also on the characteristic time constant τ_e of our (time-dependent) specific heat experiment: the deviation from the (calculated) equilibrium specific heat is found at a lower T when the system is given more time to relax. We conclude that the drop indicates that nuclear spins can no longer reach thermal equilibrium within time τ_e. We may write $c_{\mathrm{nucl}}(\tau_e) = c_{\mathrm{nucl}}^{\mathrm{eq}}[1 - \exp(-\tau_e/T_1)]$, showing that the transition should occur when the nuclear spin-lattice relaxation time T_1 becomes of the order of τ_e. These transitions to nonequilibrium provide therefore direct information on the temperature and field dependence of T_1, which can be related to the fluctuation of the transverse hyperfine field, as produced by the phonon-induced transitions between different levels of the electronic spin [16].

At low T and high B, only the ground and the first excited states, $m = +12$ and $m = +11$, need be considered. We may write $1/T_1 \simeq (1/\tau_0)\exp\{-[g\mu_B B]/k_B T\}$, where $1/\tau_0$ plays the role of an attempted frequency for the electron-spin transitions. Clearly, the nuclear spins can be taken out of equilibrium either by decreasing T down to T_B at constant field (as in Fig. 4) or by increasing B up to a given value B_B at constant T. This is indeed observed experimentally (not shown). The effect of the field is just to polarize the electronic spins, which reduces the fluctuations of the hyperfine field, thus effectively disconnecting nuclear spins from the lattice. For a given τ_e, B_B must increase linearly with T_B, which is confirmed by the experimental data plotted in the inset of Fig. 4. The slope gives $\tau_0 \approx 3 \times 10^{-4}\,\mathrm{s}$. Using this value, we have calculated the time-dependent c_{nucl}, shown as the full lines in Fig. 4, and seen to be in reasonable agreement with the experimental data at all T and B.

*To whom all correspondence should be addressed. Email address: dejongh@phys.leidenuniv.nl

[1] S. J. White, M. R. Roser, J. Xu, J. T. van Noordaa, and L. R. Corruccini, Phys. Rev. Lett. **71**, 3553 (1993).

[2] See, e.g., D. Bitko, T. F. Rosenbaum, and G. Aeppli, Phys. Rev. Lett. **77**, 940 (1996); G. Mennenga, L. J. de Jongh, and W. J. Huiskamp, J. Magn. Magn. Mater. **44**, 59 (1984).

[3] J. F. Fernández and J. J. Alonso, Phys. Rev. B **62**, 53 (2000); J. F. Fernández, Phys. Rev. B **66**, 064423 (2002).

[4] C. Sangregorio, T. Ohm, C. Paulsen, R. Sessoli, and D. Gatteschi, Phys. Rev. Lett. **78**, 4645 (1997).

[5] S. M. Aubin, N. R. Dilley, L. Pardi, J. Krzystek, M. W. Wemple, L.-C. Brunel, M. B. Maple, G. Christou, and D. N. Hendrickson, J. Am. Chem. Soc. **120**, 4991 (1998).

[6] L. Thomas, A. Caneschi, and B. Barbara, Phys. Rev. Lett. **83**, 2398 (1999).

[7] F. L. Mettes, F. Luis, and L. J. de Jongh, Phys. Rev. B **64**, 174411 (2001); F. Luis, F. L. Mettes, J. Tejada, D. Gatteschi, and L. J. de Jongh, Phys. Rev. Lett. **85**, 4377 (2000); F. L. Mettes, G. Aromí, F. Luis, M. Evangelisti, G. Christou, D. Hendrickson, and L. J. de Jongh, Polyhedron **20**, 1459 (2001).

[8] G. Aromí, M. J. Knapp. J.-P. Claude, J. C. Huffman, D. N. Hendrickson, and G. Christou, J. Am. Chem. Soc. **121**, 5489 (1999).

[9] We have used the crystallographic data for a related complex $\mathrm{Mn}_6\mathrm{O}_4\mathrm{Cl}_4(\mathrm{Et}_2\mathrm{dbm})_6$ [8], in which the Br^- ions are replaced by Cl^-.

[10] A. Bencini and D. Gatteschi, *EPR of Exchange Coupled Systems* (Springer-Verlag, Berlin and Heidelberg, 1990).

[11] The electronic specific heat was obtained by subtracting from the total specific heat the contribution of the lattice, which follows the well-known Debye approximation for low temperatures $c_{\mathrm{latt}} \propto (T/\Theta_D)^3$, where $\Theta_D \simeq 48\,\mathrm{K}$, as well as the contribution c_{nucl} arising from the nuclear spins, as discussed in the text.

[12] J. F. Fernández and F. Luis (unpublished).

[13] See, e.g., L. J. de Jongh and A. R. Miedema, Adv. Phys. **50**, 947 (2001).

[14] A. Abragam and A. Bleaney, *Electron Paramagnetic Resonance of Transition Ions* (Clarendon Press, Oxford, 1970).

[15] M. Zheng and G. C. Dismukes, Inorg. Chem. **35**, 3307 (1996).

[16] A. Abragam, *The Principles of Nuclear Magnetism* (Clarendon Press, Oxford, 1961). For a recent application of the theory to Mn_{12}, see Y. Furukawa *et al.*, Phys. Rev. B **64**, 104401 (2001).